

# Infrared Multiple-Photon Dissociation Mechanisms of Peptides of Glycine

Ronghu Wu and Terry B. McMahon<sup>\*[a]</sup>

Since the introduction of soft ionization techniques, such as electrospray ionization (ESI)<sup>[1]</sup> and matrix-assisted laser desorption/ionization (MALDI),<sup>[2,3]</sup> to generate intact peptide and protein ions in the gas phase for mass-spectrometric investigations,<sup>[4–6]</sup> fragmentation of protonated peptides and proteins has become one of the most important methods for characterization of their amino acid sequence. Therefore it is of considerable interest to understand the dissociation pathways and mechanisms for protonated peptides.<sup>[7,8]</sup> Several models, for example the mobile-proton model<sup>[9]</sup> and the pathways-in-competition model,<sup>[7]</sup> have been put forward to explain the experimental results. The observed fragmentation pattern depends on many diverse elements, including the amino acid composition, size of the peptide, charge of the molecule, translational energy and other instrumental parameters, which results in the dissociation mechanism being very complex. Many activation methods have been used to dissociate peptide and protein ions, such as collision-induced dissociation (CID),<sup>[10]</sup> surface-induced dissociation (SID),<sup>[11]</sup> electron-capture dissociation (ECD),<sup>[12]</sup> black-body infrared dissociation (BIRD)<sup>[13,14]</sup> and infrared multiple-photon dissociation (IRMPD). IRMPD, as a low-energy activation method, has attracted heightened interest recently,<sup>[15–20]</sup> and IRMPD vibrational spectroscopy is also a very powerful technique to clearly elucidate the structures of gas-phase ions in combination with electronic-structure calculations.<sup>[21–27]</sup> However, to date, the IRMPD mechanism has not been unambiguously understood. The mode-selective IRMPD described in the present work provides a further insight into the peptide dissociation mechanism.

In the present work, the IRMPD pathways and mechanisms for protonated glycine and the series of protonated oligomers (GlyGly, GlyGlyGly, GlyGlyGlyGly and GlyGlyGlyGlyGly) have been investigated. The combination of a free-electron laser (FEL) and ion-trap mass spectrometers

or Fourier transfer ion-cyclotron mass spectrometers (FTICR) has been demonstrated to be a very powerful tool for the investigation of the IRMPD mechanism of peptides. This high-intensity IR source may be tuned precisely to a given wavelength corresponding to a particular vibrational mode, such that initial mode-specific activation may be accomplished. This then permits the question to be addressed of whether the initial protonation site or the different conformations of a peptide will have any effect on the dissociation pathway of the peptide and whether there is any difference in dissociation pathways when different vibrational modes are activated. Without any side chains, Gly<sub>n</sub> forms the backbone of peptides and proteins. Thus they may serve well as a model to understand the structures and properties of peptides and proteins.

By scanning the wavelength of the IR laser, IRMPD vibrational spectra are obtained that can then be used to determine the optimal wavelength to activate the protonated oligomers of glycine. For example, the decomposition spectrum of the parent ion of protonated GlyGly is shown in Figure 1, together with the two fragment ion spectra at *m/z*

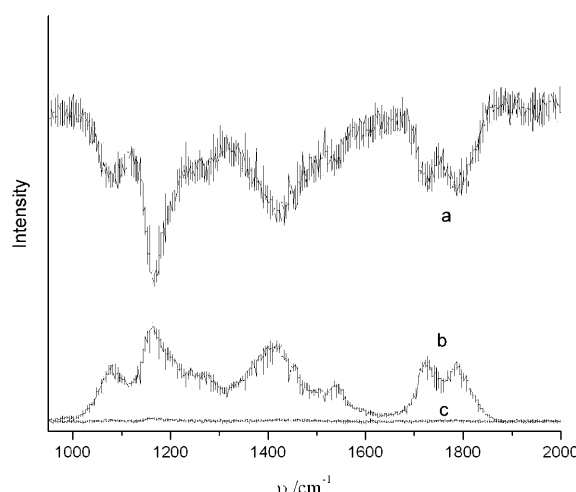


Figure 1. Change in intensities as a function of IR laser wavelength for a) the parent ion of GlyGlyH<sup>+</sup> (*m/z* 133) and b) the *m/z* 76 and c) *m/z* 88 fragment ions.

[a] Dr. R. Wu, Prof. T. B. McMahon  
Department of Chemistry, University of Waterloo  
Waterloo, Ontario, N2L 3G1 (Canada)  
Fax: (+1) 519-746-0435  
E-mail: mcmahon@uwaterloo.ca

76 and 88. In these spectra, ten replicates at every wavelength have been recorded and each of the ten intensities are displayed, with no averaging, leading to the scattered appearance of the data. It can be seen that each dip in the decomposition spectrum of the parent ion is directly related to the increase in the intensity of a fragment ion. Across the entire wavelength range studied, the signal intensity of the fragment peak at  $m/z$  76 is clearly stronger than that at  $m/z$  88 (to be discussed below).

The IRMPD vibrational spectrum, expressed as the fragmentation efficiency,  $P_{\text{frag}}$  ( $P_{\text{frag}} = -\ln[I_{\text{parent}}/(I_{\text{parent}} + \sum I_{\text{fragment}})]$ ), as a function of the photon energy, in  $\text{cm}^{-1}$ , is shown in Figure 2. This spectrum is a sensitive probe of the structure of the parent ions. To assign the bands, the calculated spectra of the two most energetically favourable, yet structurally distinct, stable isomers are included.

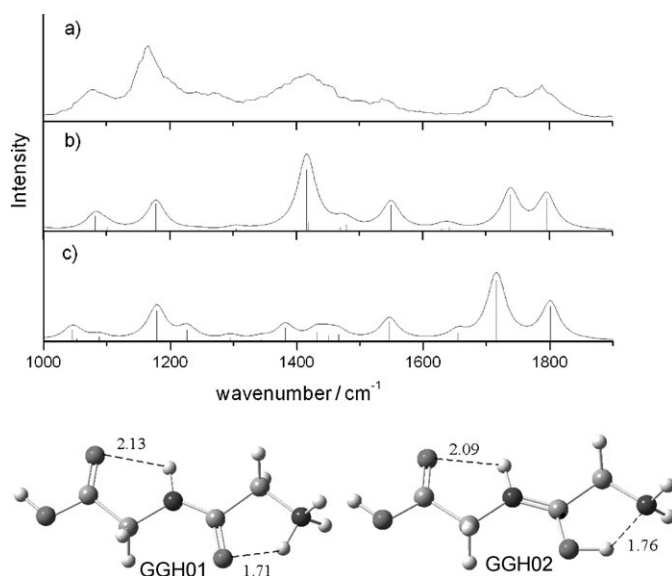


Figure 2. a) IRMPD vibrational spectrum of protonated GlyGly and the calculated spectra of the two most stable isomers: b) GGH01 and c) GGH02.

In GGH01, the most stable isomer, the proton is bound to the amino nitrogen atom and a hydrogen bond is formed between one of the acidic hydrogen atoms of the resulting ammonium group and the amide oxygen. The amide NH forms a second hydrogen bond with the carboxyl oxygen atom. At the B3LYP/6-311+G(d, p) level of theory,<sup>[28]</sup> GGH01 is  $1.2 \text{ kcal mol}^{-1}$  more stable in free energy at 298 K than GGH02, in which a proton is bound to an amide oxygen with two resulting intramolecular hydrogen bonds. As seen in Figure 2, the experimental IRMPD spectrum is in very good agreement with that calculated for GGH01. The weak band at  $1077 \text{ cm}^{-1}$  corresponds to the amide CN stretch, and the strongest band at  $1166 \text{ cm}^{-1}$  can be assigned to the bending vibration of the hydroxyl group. These are consistent with the calculated values of  $1077$  and  $1172 \text{ cm}^{-1}$  for GGH01, respectively. The umbrella vibration of  $-\text{NH}_3$  ap-

pears at  $1418 \text{ cm}^{-1}$ , which fits very well with the calculated value of  $1409 \text{ cm}^{-1}$ . The band at  $1540 \text{ cm}^{-1}$  corresponds to that calculated for the NH bending of the amide group (the amide II mode) at  $1542 \text{ cm}^{-1}$ . The bands at  $1722$  and  $1788 \text{ cm}^{-1}$  correspond to the amide I modes (the carbonyl stretching vibrations), which are in excellent agreement with the calculated values of  $1729$  and  $1786 \text{ cm}^{-1}$  for this mode in the amide and carboxylic acid groups, respectively. According to the calculated energies, presuming a Boltzmann distribution of possible isomers, the amounts of GGH01 and GGH02 would be 98.0 and 2.0%, respectively. Examination of the experimental IRMPD spectrum leads to the conclusion that, while the presence of GGH02 cannot be excluded, the most stable isomer, GGH01, is clearly the dominant species.

In the IRMPD mass spectra shown in Figure 3, the laser wavelength has been fixed at the carbonyl stretching mode for each of the protonated glycine oligomers investigated.

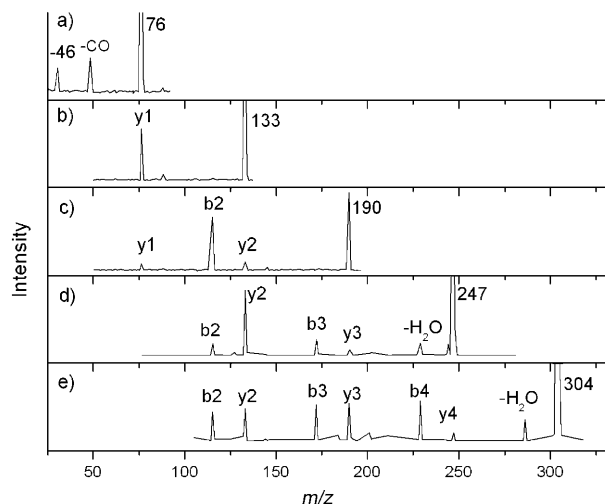
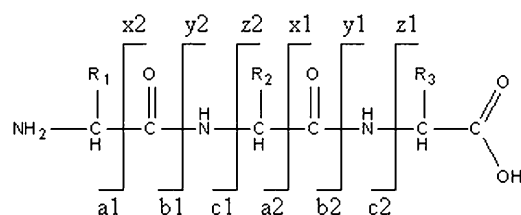


Figure 3. IRMPD mass spectra of the protonated glycine and its peptides: a) Gly, b) GlyGly, c) GlyGlyGly, d) GlyGlyGlyGly and e) GlyGlyGlyGlyGly.

For protonated glycine, the main fragment peak at  $m/z$  48 corresponds to the loss of CO with a somewhat weaker peak from the loss of 46 u. The fragmentation of  $\text{GlyH}^+$  has been extensively investigated by different experimental and computational methods.<sup>[29–33]</sup> Using CID, the main fragmentation corresponds to the loss of 46 u with only a minor fragment appearing at  $m/z$  48. Hoppiliard et al.<sup>[31]</sup> investigated several different dissociation pathways using theoretical calculations and, according to their results, the barriers for loss of  $\text{HCOOH}$ ,  $\text{C}(\text{OH})_2$  or  $\text{CO}_2 + \text{H}_2$  are 90.3, 74.8 and  $72.9 \text{ kcal mol}^{-1}$ , respectively. However, the barriers for the loss of CO or sequential loss of CO and water are identical at  $36.6 \text{ kcal mol}^{-1}$ . When protonated glycine loses ammonia, the calculated energy barrier is  $78.0 \text{ kcal mol}^{-1}$ . From these data, the authors concluded that the loss of  $\text{HCOOH}$  or  $\text{C}(\text{OH})_2$  under low-energy collision conditions is impossible and thus the loss of 46 u must correspond to the loss of CO

and water. The fragmentation of protonated glycine by loss of CO and water requires proton transfer from the amino to the hydroxyl group, which yields an intermediate that can either eliminate CO + H<sub>2</sub>O or CO, depending upon the lifetime of the intermediate(s), which is determined by the specific experimental conditions. The low-energy CID spectrum shows a dominant loss of CO + H<sub>2</sub>O with a minor loss of CO.<sup>[29,30]</sup> In contrast, in the metastable ion spectrum of FAB- and CI-generated protonated glycine, CO loss is the almost exclusive dissociation channel.<sup>[32,33]</sup> In the current IRMPD spectrum, the losses of CO and CO + H<sub>2</sub>O are both observed in an approximate 3:2 ratio. According to the calculated energy barrier of 36.6 kcal mol<sup>-1</sup>,<sup>[29]</sup> roughly seven photons at 1750 cm<sup>-1</sup> are required to dissociate the protonated glycine. The energy of the products in the CO + H<sub>2</sub>O loss channel lies only 5.6 kcal mol<sup>-1</sup> below the overall reaction barrier. This means that if the departing CO molecule carries off one (~6 kcal mol<sup>-1</sup>) or more vibrational quanta, the subsequent loss of H<sub>2</sub>O will become endothermic. This indicates that IRMPD is a very low-energy activation method.

For a protonated peptide, if fragmentation occurs at the C–N bond of a peptide linkage and if the charge is retained on the N-terminal fragment, a b ion is produced; if the charge is on the C-terminal fragment, a y ion forms after proton migration from the N-terminal to the C-terminal product, as shown in Scheme 1. Other product ions, includ-



Scheme 1.

ing the a ions, internal iminium (immonium) ions (that originate from non-terminal residues) and ions that result from the loss of small neutral molecules, for example, CO, H<sub>2</sub>O, and NH<sub>3</sub>, may also be formed from the fragmentation of the protonated peptide or from its charged products.<sup>[8]</sup>

In the IRMPD spectrum of protonated GlyGly, the dominant fragment appears at *m/z* 76 (y1 fragment). In addition, there is a very small peak at *m/z* 88, corresponding to the loss of CO and ammonia. Van Dongen et al.<sup>[34]</sup> found that fragmentation of protonated GlyGly includes y1 (72%), a1 (17%) and b2 (5%) ions as well as loss of CO (6%) by using low-energy CID. However, in the present IRMPD spectrum, the peak corresponding to the loss of CO is almost negligible. Quantum-chemical and RRKM (Rice–Ramsperger–Kassel–Marcus) calculations have been carried out on protonated GlyGly to understand the main fragmentation pathways leading to formation of a1 and y1 ions. Two possible mechanisms<sup>[35]</sup> were considered. The first pathway

results in elimination of aziridinone as a neutral counterpart of the y1 ion formed, in which the nitrogen atom in the N-terminal group attacks the positive carbon atom and forms the aziridinone, a three-membered-ring species. The second, “a1–y1”, pathway leads to simultaneous formation of a1 and y1 ions. The calculated results showed that the “a1–y1” pathway has a much lower threshold energy (38.0 kcal mol<sup>-1</sup>) than that of the “aziridinone” formation (48.6 kcal mol<sup>-1</sup>). Furthermore, the “a1–y1” pathway is more kinetically favourable over the entire internal energy range than that for “aziridinone” formation. The elimination of water from the carboxyl group of protonated GlyGly has also been investigated by density functional theory calculations.<sup>[36]</sup> Although the threshold energy for b2 ion formation (37.1 kcal mol<sup>-1</sup>) is slightly lower than that for the y1 ion (38.4 kcal mol<sup>-1</sup>), the former requires a tight transition state with an activation entropy of –1.2 cal mol<sup>-1</sup> K<sup>-1</sup>, while the latter has a loose transition state with a +8.8 cal mol<sup>-1</sup> K<sup>-1</sup> entropy change. This leads to y1 being the major fragment ion over a wide energy range, consistent with the present experimental results.

For the protonated GlyGlyGly, the main fragment is b2, consistent with previous observations.<sup>[37,38]</sup> There is a popular and reasonable mechanism for the formation of the b2 ion for protonated GlyGlyGly. After activation, it is energetically feasible for the proton to migrate from one position to another. When the proton resides on an amide group adjacent to the N terminus, the amide oxygen atom at the N terminus attacks the carbonyl carbon atom of the second amide bond, thereby forming a transition state comprised of an incipient oxazolone (the b2 ion) and an incipient (neutral) glycine. The products then separate to give the b2 ion, and glycine. As can be seen from Figure 3, both y2 and y1 also appear. Their intensities are markedly weaker than that of b2; however, y2 is stronger than y1. This is consistent with the previous results in which the onset energy of y2 is evidently lower than that of y1.<sup>[29]</sup> The formation of y1 is due to the cleavage of the same amide bond as in formation of b2. The much stronger b2 peak can be attributed to the fact that the proton affinity of the corresponding neutral for b2 is higher than that for y1, that is, glycine.

The main fragment of protonated GlyGlyGlyGly is y2. The y2 and b2 ions are both due to the cleavage of the same middle amide bond. Klassen et al.<sup>[29]</sup> have observed much slower dissociation kinetics for cleavage of the amide bonds at either end of the peptide compared with the middle bond. In contrast to GlyGlyGly, here y2 is evidently the stronger peak, in which the proton affinity of the corresponding neutral for b2 is less than that for y2, that is, diglycine. This has also been confirmed by calculations, in which the proton affinity of the neutral for b2 is 217.4 kcal mol<sup>-1</sup> at the B3LYP/6-311+G(d, p) level of theory, and the proton affinities of Gly and GlyGly are 211.5 and 219.2 kcal mol<sup>-1</sup>, respectively. The calculated value for Gly is also consistent with that of 211.9 kcal mol<sup>-1</sup> in the NIST database. In addition, b3 and y3 ions are minor fragments, and the small peak at *m/z* 229 is due to the loss of water.

For the protonated GlyGlyGlyGlyGly, peaks corresponding to b2, b3, b4, y2 and y3 ions all appear. The b2/y3 and b3/y2 pairs are each due to the cleavage of the same amide bonds, respectively. In the CID spectrum,<sup>[39]</sup> the main peaks are the b4 ion and the loss of water. Other peaks, such as b2, y2, b3 and y3, are much weaker than b4. In the present spectrum, b2, b3, b4, y2 and y3 have almost the same intensities. This happens not only at 1745 cm<sup>-1</sup>, but also at other frequencies, such as 1230 and 1540 cm<sup>-1</sup> as well as others. From these phenomena, it may be inferred that the barriers for the different decomposition channels, that is, the cleavage of the amide bonds (with the exception of the first amide bond adjacent to the N terminus) are very similar, with an energy difference of less than the energy of one 1750 cm<sup>-1</sup> photon (~5 kcal mol<sup>-1</sup>). In addition, dissociation leading to a proton resident on either the N-terminal or C-terminal fragment has nearly the same probability. For example, the b2 and y3 pair as well as b3 and y2 pair are nearly equal in intensity, which implies that the product signals may not be controlled by a statistical distribution. This possibility clearly requires further study.

Reid et al. have investigated the fragmentation of oligomers of glycine<sup>[39]</sup> using CID and found that for tetra- and pentaglycine the MS/MS spectra reveal major losses of neutral water. However, in the IRMPD spectra, although the peaks corresponding to the loss of water appear, the intensities are much lower and the main fragment pathways are due to the cleavage of the amide bonds. This then indicates that IRMPD forms the more structurally informative b and y sequence ions and fewer, less useful, non-sequence ions formed by loss of small neutrals such as water and ammonia.

To investigate the effect of activating different vibrational modes on the fragmentation, the corresponding IRMPD spectra of protonated GlyGly obtained at different activation wavelengths are shown in Figure 4. The modes at 1163, 1416, 1727 and 1788 cm<sup>-1</sup> correspond to the bending vibra-

tion of the hydroxyl group, the umbrella vibration of -NH<sub>3</sub> and the two carbonyl stretching vibrations, respectively. From these spectra, it is apparent that the decomposition mechanisms are the same at the different activation wavelengths, although the decomposition efficiencies are different, because the absorption intensities, the laser intensities and the energies of the photons are different at these wavelengths, in accord with the data shown in Figure 2.

It is of interest to speculate whether the initial protonation sites or different conformations give rise to different dissociation mechanisms. It has been previously reported that b- and y-type "sequence ions" formed by CID may be influenced not only by the initial site of protonation, but also by the proton affinities of the fragments formed, peptide conformation and competing neighbouring group participation reactions leading to the formation of "non-sequence" ion structure.<sup>[39]</sup> This conjecture is addressed below.

Combined with the theoretical calculations, the experimental IRMPD spectra of GlyGlyGlyH<sup>+</sup> indicate clearly that two main isomers co-exist under the present experimental conditions.<sup>[40]</sup> These two isomers have totally different protonation sites and conformations. One isomer is a linear structure with a proton bound to an amide oxygen atom, and the protonation site of the other, cyclic, isomer is at the amino nitrogen atom. Consequently they have different vibrational spectra. Here the two modes at 1803 and 1745 cm<sup>-1</sup> have been selected to activate and dissociate the two different isomers of the protonated GlyGlyGly. The vibration at 1803 cm<sup>-1</sup> corresponds to the carbonyl stretching of the linear isomer and that at 1745 cm<sup>-1</sup> is due to the same mode of the cyclic isomer. The IRMPD mass spectra are shown in Figure 5. These two spectra are almost identical, with the exception that the fragments in the spectrum at 1745 cm<sup>-1</sup> are slightly stronger, which is due to the stronger absorption. These experimental results indicate very clearly that the dissociation mechanism is not related to the initial protonation site or peptide conformation.

IRMPD is a relatively new activation method with considerable potential to reveal both structural and energetic information for peptides and proteins. By using a very powerful wavelength-tunable FEL combined with ion-trap mass spectrometry, IRMPD mechanisms of protonated peptides of glycine (Gly<sub>1-5</sub>H<sup>+</sup>) have been investigated. The experimental results indicate that the main fragmentation pathways of the peptides are due predominantly to the cleavage of the amide bond. Compared with traditional low-energy collision-induced dissociation, IRMPD forms more structurally informative sequence b and y ions, and fewer less useful non-sequence ions from the loss of small neutrals such as water and ammonia. It is found clearly that the dissociation pathways are the same through excitation of different modes of the peptide. For the first time, it has thus been confirmed that the peptide dissociation pathway is not related to the initial protonation site or the conformation of the peptide. A further understanding of the dissociation mechanism of peptides will aid in determination of sequence in peptides and proteins of large size.

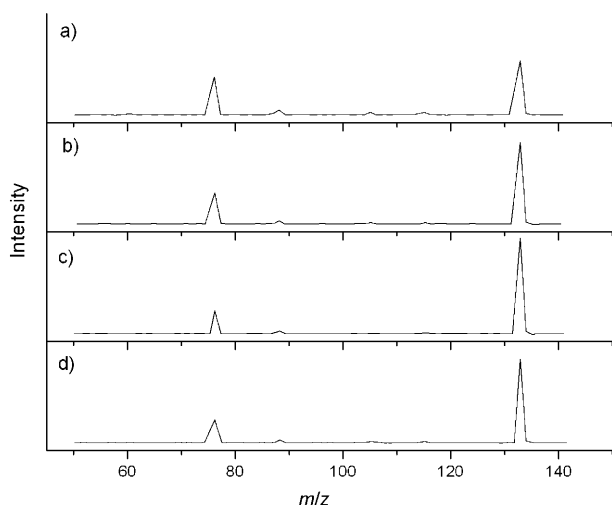


Figure 4. IRMPD mass spectra of GlyGlyH<sup>+</sup> obtained via exciting the different modes: a) 1163, b) 1416, c) 1727 and d) 1788 cm<sup>-1</sup>.

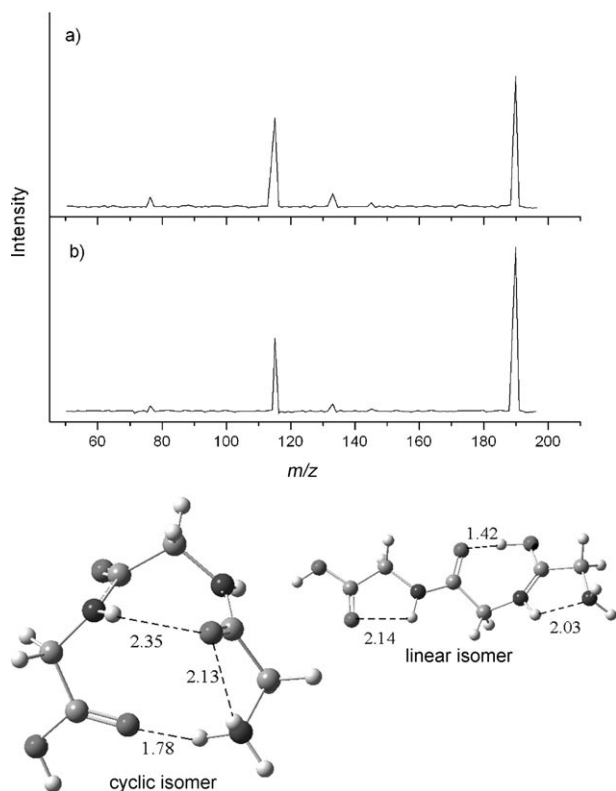


Figure 5. IRMPD mass spectra of the different isomers of protonated GlyGlyGly with different initial protonation sites and conformations: a) the cyclic isomer activated at  $1745\text{ cm}^{-1}$  and b) the linear isomer activated at  $1803\text{ cm}^{-1}$ .

## Experimental Section and Computational Methods

Experiments have been carried out using the free-electron laser (FEL) at the Centre de Laser Infrarouge d'Orsay (CLIO) facility in Orsay (France) coupled to an electrospray ionization ion-trap mass spectrometer (Bruker Esquire3000+). This experimental configuration has been described in detail previously.<sup>[26,27]</sup> The FEL facility is based on emission from a 10–50 MeV electron beam. For the high-energy electron beam, the emission photon wavelength could be tuned by adjusting the gap of the undulator, which was placed in the optical cavity. In the present work, the electron energy was set to 48 MeV in order to adjust and scan the wavelength from 1000 to  $2000\text{ cm}^{-1}$ . The IR-FEL output consisted of macropulses  $8\text{ }\mu\text{s}$  in length with a repetition rate of 25 Hz. Each macropulse involved approximately 500 micropulses with a width of a few picoseconds. For a typical average IR power of 500 mW, the corresponding micropulse and macropulse energies are about  $40\text{ }\mu\text{J}$  and  $20\text{ mJ}$ , respectively.

To produce protonated species of glycine and its oligomer, a  $10^{-5}\text{ M}$  solution of the sample dissolved in a mixture of water and methanol, with a very small amount of formic acid, was used. The desired ion was isolated and confined in the ion trap for the controlled period of time, during which the IR laser beam, tuned to a desired wavelength, was introduced into the ion trap to dissociate the isolated ion. Mass spectra were then recorded to probe dissociation. The IRMPD vibrational spectrum was measured by scanning the wavelength in steps of  $\sim 4\text{ cm}^{-1}$ .

Theoretical calculations were carried out with the Gaussian 03 program package.<sup>[28]</sup> The structures of the protonated peptides were optimized at the density functional theory (DFT) level, by employing the B3LYP exchange-correlation functional and the 6-311+G(d, p) basis set. The calculated harmonic vibrational frequencies have been determined using the same method, scaled by a factor of 0.99. The calculated frequencies and

intensities were convoluted assuming a Lorentzian profile with a  $35\text{ cm}^{-1}$  full-width at half-maximum.

## Acknowledgements

The generous financial support by the Natural Sciences and Engineering Research Council of Canada (NSERC) is gratefully acknowledged as is the financial support of the European Commission through the NEST/ADVENTURE program (EPITOPES, Project No. 15637). We are very grateful for the valuable assistance of the CLIO team, P. Maitre, J. Lemaire, J. M. Bakker, T. Besson, D. Scuderi and J. M. Ortega.

**Keywords:** fragmentation mechanism • glycine • IRMPD (infrared multiple-photon dissociation) • mass spectrometry • peptides

- [1] J. B. Fenn, M. Mann, C. K. Meng, S. F. Wong, C. M. Whitehouse, *Science* **1989**, *246*, 64–71.
- [2] K. Tanaka, H. Waki, Y. Ido, S. Akita, Y. Yoshida, T. Yoshida, *Rapid Commun. Mass Spectrom.* **1988**, *2*, 151–153.
- [3] M. Karas, F. Hillenkamp, *Anal. Chem.* **1988**, *60*, 2299–2301.
- [4] J. R. Yates III, *J. Mass Spectrom.* **1998**, *33*, 1–9.
- [5] R. Aebersold, M. Mann, *Nature* **2003**, *422*, 198–207.
- [6] X. M. Han, K. Breuker, F. W. McLafferty, *Science* **2006**, *314*, 109–112.
- [7] B. Bogdanov, R. D. Smith, *Mass Spectrom. Rev.* **2005**, *24*, 168–200.
- [8] B. Paizs, S. Suhai, *Mass Spectrom. Rev.* **2005**, *24*, 508–548.
- [9] V. H. Wysocki, G. Tsaprailis, L. L. Smith, L. A. Brechi, *J. Mass Spectrom.* **2000**, *35*, 1399–1406.
- [10] J. Laskin, J. H. Futrell, *Mass Spectrom. Rev.* **2003**, *22*, 158–181.
- [11] V. H. Wysocki, K. A. Resing, Q. F. Zhang, G. L. Cheng, *Methods* **2005**, *35*, 211–222.
- [12] H. J. Cooper, K. Hakansson, A. G. Marshall, *Mass Spectrom. Rev.* **2005**, *24*, 201–222.
- [13] R. C. Dunbar, T. B. McMahon, *Science* **1998**, *279*, 194–197.
- [14] D. S. Gross, Y. X. Zhao, E. R. Williams, *J. Am. Soc. Mass Spectrom.* **1997**, *8*, 519–524.
- [15] S. K. Shin, J. L. Beauchamp, *J. Am. Chem. Soc.* **1990**, *112*, 2057–2066.
- [16] D. P. Little, J. P. Speir, M. W. Senko, P. B. Oconnor, F. W. McLafferty, *Anal. Chem.* **1994**, *66*, 2809–2815.
- [17] D. S. Tonner, T. B. McMahon, *Anal. Chem.* **1997**, *69*, 4735–4740.
- [18] E. D. Dodds, P. J. Hagerman, C. B. Lebrilla, *Anal. Chem.* **2006**, *78*, 8506–8511.
- [19] N. C. Polfer, J. J. Valle, D. T. Moore, J. Oomens, J. R. Eyler, B. Bendiak, *Anal. Chem.* **2006**, *78*, 670–679.
- [20] J. J. Wilson, J. S. Brodbelt, *Anal. Chem.* **2007**, *79*, 2067–2077.
- [21] G. von Helden, D. van Heijnsbergen, G. Meijer, *J. Phys. Chem. A* **2003**, *107*, 1671–1688.
- [22] L. MacAleese, P. Maitre, *Mass Spectrom. Rev.* **2007**, *26*, 583–605.
- [23] R. H. Wu, T. B. McMahon, *J. Am. Chem. Soc.* **2007**, *129*, 4864–4865.
- [24] R. H. Wu, T. B. McMahon, *Angew. Chem.* **2007**, *119*, 3742–3745; *Angew. Chem. Int. Ed.* **2007**, *46*, 3668–3671.
- [25] N. C. Polfer, J. Oomens, S. Suhai, B. Paizs, *J. Am. Chem. Soc.* **2007**, *129*, 5887–5897.
- [26] J. Lemaire, P. Boissel, M. Heninger, G. Mauclaire, G. Bellec, H. Mestdagh, A. Simon, S. Le Caer, J. M. Ortega, F. Glotin, P. Maitre, *Phys. Rev. Lett.* **2002**, *89*, 273002.
- [27] P. Maitre, S. Le Caer, A. Simon, W. Jones, J. Lemaire, H. Mestdagh, M. Heninger, G. Mauclaire, P. Boissel, R. Prazeres, F. Glotin, J. M. Ortega, *Nuclear Instrum. Methods Phys. Res. Sect. A* **2003**, *507*, 541–546.
- [28] Gaussian 03 (Revision B.03), M. J. Frisch, G. W. Trucks, H. B. Schlegel, G. E. Scuseria, M. A. Robb, J. R. Cheeseman, J. A. Montgomery-

- y Jr., T. Vreven, K. N. Kudin, J. C. Burant, J. M. Millam, S. S. Iyengar, J. Tomasi, V. Barone, B. Mennucci, M. Cossi, G. Scalmani, N. Rega, G. A. Petersson, H. Nakatsuji, M. Hada, M. Ehara, K. Toyota, R. Fukuda, J. Hasegawa, M. Ishida, T. Nakajima, Y. Honda, O. Kitao, H. Nakai, M. Klene, X. Li, J. E. Knox, H. P. Hratchian, J. B. Cross, C. Adamo, J. Jaramillo, R. Gomperts, R. E. Stratmann, O. Yazyev, A. J. Austin, R. Cammi, C. Pomelli, J. W. Ochterski, P. Y. Ayala, K. Morokuma, G. A. Voth, P. Salvador, J. J. Dannenberg, V. G. Zakrzewski, S. Dapprich, A. D. Daniels, M. C. Strain, O. Farkas, D. K. Malick, A. D. Rabuck, K. Raghavachari, J. B. Foresman, J. V. Ortiz, Q. Cui, A. G. Baboul, S. Clifford, J. Cioslowski, B. B. Stefanov, G. Liu, A. Liashenko, P. Piskorz, I. Komaromi, R. L. Martin, D. J. Fox, T. Keith, M. A. Al-Laham, C. Y. Peng, A. Nanayakkara, M. Challacombe, P. M. W. Gill, B. Johnson, W. Chen, M. W. Wong, C. Gonzalez, J. A. Pople, Gaussian, Inc., Pittsburgh, PA, **2004**.
- [29] J. S. Klassen, P. Kebarle, *J. Am. Chem. Soc.* **1997**, *119*, 6552–6563.
- [30] F. Rogalewicz, Y. Hoppilliard, G. Ohanessian, *Int. J. Mass Spectrom.* **2000**, *195/196*, 565–590.
- [31] F. Rogalewicz, Y. Hoppilliard, *Int. J. Mass Spectrom.* **2000**, *199*, 235–252.
- [32] W. Kulik, W. Heerma, *Biomed. Environ. Mass Spectrom.* **1988**, *15*, 419–427.
- [33] S. Beranova, J. Cai, C. Wesdemiotis, *J. Am. Chem. Soc.* **1995**, *117*, 9492–9501.
- [34] W. D. van Dongen, W. Heerma, J. Haverkamp, C. G. de Koster, *Rapid Commun. Mass Spectrom.* **1996**, *10*, 1237–1239.
- [35] B. Paizs, S. Suhai, *Rapid Commun. Mass Spectrom.* **2001**, *15*, 651–663.
- [36] B. Balta, V. Aviyente, C. Lifshitz, *J. Am. Soc. Mass Spectrom.* **2003**, *14*, 1192–1203.
- [37] H. E. Aribi, C. F. Rodriguez, D. R. P. Almeida, Y. Ling, W. W.-N. Mak, A. C. Hopkinson, K. W. M. Siu, *J. Am. Chem. Soc.* **2003**, *125*, 9229–9236.
- [38] B. Paizs, S. Suhai, *Rapid Commun. Mass Spectrom.* **2001**, *15*, 2307–2323.
- [39] G. E. Reid, R. J. Simpson, R. A. O'Hair, J. *Int. J. Mass Spectrom.* **1999**, *190/191*, 209–230.
- [40] R. H. Wu, T. B. McMahon, *J. Am. Chem. Soc.* **2007**, *129*, 11312–11313.

Received: March 31, 2008  
Published online: July 11, 2008